

RESEARCH PAPER RP1636

Part of *Journal of Research of the National Bureau of Standards*, Volume 34,
February 1945

REGION OF USABLE IMAGERY IN AIRPLANE- CAMERA LENSES

By Francis E. Washer

ABSTRACT

The proper positioning of a lens with respect to the focal plane in a fixed-focus camera, such as an airplane-mapping camera, is governed by several factors that relate to the optical qualities of the lens. These factors are quality of imagery, depth of focus at a given stop opening, and curvature of field. This investigation shows that there is reasonably good agreement between observed depth of focus at a given stop opening and that predicted on the basis of geometric optics. Observed values of the maximum resolving power at various angular separations from the axis are generally lower at the larger stop openings than values predicted on the basis of physical optics. This lowering is doubtless a consequence of residual aberrations, inherent in an actual lens, which are more noticeable at large aperture ratios. A method of presenting the resolving power characteristics throughout the range of useful imagery in the form of sets of master curves has been developed. These curves show at a glance the variation of resolving power with distance from the plane of best axial imagery, the depth of focus for any observed value of the resolving power, the effect of field curvature on imagery in any given image plane, and the differing performance for tangential and radial imagery at various angular separations from the axis. Successive groups of these master curves show how variations in stop opening affect the performance of a lens.

CONTENTS

	Page
I. Introduction.....	175
II. Method.....	176
III. Theory.....	177
1. Maximum resolving power of an ideal lens.....	177
2. Depth of focus for an ideal lens.....	178
IV. Results of measurement.....	180
1. Variation in depth of focus on the axis with stop opening.....	187
2. Variation in resolving power on the axis with stop opening.....	191
3. Effect of field curvature.....	192
4. Change in depth of focus with angular separation from the axis.....	193
5. Change in maximum resolving power with angular separation from the axis.....	195
6. Variation of resolving power in a given image plane with stop opening.....	197

I. INTRODUCTION

In the use of aerial photographs for mapping, the quality of definition is of considerable importance. Since quality of definition in a photograph is directly related to the resolving power of the lens used

in the aerial camera, the factors affecting resolving power throughout the entire area of the image plane are of special interest. These factors are depth of focus, stop opening, and curvature of field. All of these factors are considered in the proper positioning of the lens in the camera. For a lens free from aberration, the image plane of best definition is unique and its position can readily be determined theoretically, but for an actual lens it is necessary to resort to experiment and to compromise upon a position of the lens that yields best average definition throughout the image plane. This is usually done at the maximum stop opening of the lens, and this setting is then held, in the fixed-focus airplane camera, for all smaller stop openings.

Since the position of best average definition for a lens is generally determined with the lens not mounted in a camera, and since the lens may then be mounted in such manner that the distance from rear vertex of lens to image plane (back focal length) is not that prescribed for best average definition, it is of interest to know how great a departure from the prescribed position is allowable before the deterioration of imagery becomes sufficient to impair the usefulness of the camera. These tolerances are best determined from information on the depth of focus and curvature of field of lenses used in practice. The present paper therefore shows the results of measurement on resolving power for several typical airplane camera lenses. This information is presented in such manner that the effect of depth of focus, stop opening, and curvature of field is readily apparent.

II. METHOD

The precision lens testing camera¹ is well suited to the study of the resolving power characteristics of a lens throughout the region of usable imagery. The only modification in procedure from that previously reported² is the increasing of the range through which the camera back moves in making a resolving power negative. Fifty-seven steps instead of nineteen are made, and the negative shows the resolving power at definite intervals from 6.5 mm nearer to the lens to 6.5 mm farther from the lens than the plane of best axial focus. The negatives are examined under a microscope and the resolving powers recorded for each image. A pattern is not considered resolved unless all coarser patterns are also resolved and the number of lines in the resolved patterns agree with that of the corresponding patterns in the test chart. In this manner, the values of the resolving power are determined for each of the 57 image planes at every 5° interval from the axis from 0° to the limiting angle set by the lens. By making such a negative for each stop opening, the region of usable imagery is explored throughout the range of aperture selected.

Although a large number of lenses have been studied in this manner the results of only four are here presented, and of these four, two are selected for a more complete description. The lenses selected are representative of a wide range of focal lengths, angular fields, and function in mapping. Lens *A* is a wide angle airplane-mapping lens, nominal focal length is 150 mm, maximum aperture $f/6$, and a useful field of view 45°. Lens *B* is a lens usable in copying cameras or for general photography; it has a nominal focal length of 195 mm, maximum aperture $f/5.6$, and a normally useful field angle between 20°

¹J. Research NBS 15, 449 (1937) RP984.

²J. Research NBS 22, 729 (1939) RP1216.

and 25°. Lens *C* is usable in copying cameras or for general photography; it has a nominal focal length of 210 mm, maximum aperture $f/6.8$ and a normally useful field angle of 25°. Lens *D* is frequently used in aerial cameras and also in copying cameras; it has a nominal focal length of 125 mm, maximum aperture $f/8$, and a normally useful field angle of 35°. Lenses *A* and *B* have been selected for the fuller description of their resolving power characteristics whereas *C* and *D* are limited to a partial description.

III. THEORY

A brief discussion of the resolving power characteristics as predicted from theoretical considerations is necessary before proceeding to the results of measurements. This theory has long been established and predictions from it will be used in this article only for the purpose of providing a yardstick against which to compare the performance of the lenses studied. Since the predicted values of resolving power are for an ideal lens, it is not surprising that some apparent contradictions to the theory will be found in the experimental results. These deviations result from aberrations inherent in any actual lens. These departures do not however signify that the theory is without value in the prediction of lens performance. On the contrary, the number of times that the observed data are of the same order of magnitude as the predicted values is sufficiently high that one may feel more confident than ever that the predicted values are sufficiently close to the true values as to render them a valuable aid. This is particularly true when dealing with resolving powers of the same order of magnitude as those of the more commonly used photographic emulsions.

1. MAXIMUM RESOLVING POWER OF AN IDEAL LENS

The smallest separation of two star images theoretically obtainable on the basis of diffraction of light is

$$X = \frac{1.22F\lambda}{d} \quad (1)$$

where X is the separation, F the focal length of the lens, d the diameter of the lens and λ the wavelength of the incident light. For the purpose of the present work, it will be assumed that the same equation is valid where the images are composed of parallel lines instead of points. It is also more convenient to express the maximum resolving power, A_m , in lines per millimeter. It can be shown that the equation,

$$A_m = \frac{1426}{b} \text{ lines per millimeter,} \quad (2)$$

where b is the f -number, is equivalent to eq 1. This relation is computed for a wavelength of 575 millimicrons, which is the effective wavelength of the light used in making resolving power negatives with the precision lens-testing camera. This equation is valid only on the axis of the lens. For extra axial points, it is necessary to use the two

additional approximate relations, one for maximum resolving power for tangential lines,

$$A_{\theta} = \frac{1426}{b} \cdot \cos^3 \theta, \quad (3)$$

and another for maximum resolving power for radial lines,

$$A_{r\theta} = \frac{1426}{b} \cdot \cos \theta, \quad (4)$$

where θ is the angular separation from the axis of the point considered. Table 1 gives the values computed for the resolving power in both orientations at 5° intervals from 0° to 45° for a series of f -numbers ranging from $f/4$ to $f/64$ in a form convenient for use.

TABLE 1.—*Maximum resolving power for an ideal lens as a function of stop opening in lines per millimeter*

Relative aperture or f -number	Resolving power for tangential lines. Angular distance from axis.									
	0°	5°	10°	15°	20°	25°	30°	35°	40°	45°
4	356	352	340	321	295	265	231	196	160	126
5.6	255	252	244	230	212	190	166	140	115	90
8	178	176	170	160	148	132	116	98	80	63
11	130	128	124	117	108	97	84	71	58	46
16	89	88	85	80	74	66	58	49	40	31
22	65	64	62	58	54	48	42	36	29	23
32	45	44	43	41	37	33	29	25	20	16
45	32	32	31	29	26	24	21	18	14	11
64	22	22	21	20	18	16	14	12	10	8
	Resolving power for radial lines. Angular distance from axis.									
	0°	5°	10°	15°	20°	25°	30°	35°	40°	45°
4	356	355	351	344	334	323	308	292	273	252
5.6	255	254	251	246	240	231	221	209	195	180
8	178	177	175	172	167	161	154	146	136	126
11	130	130	128	126	122	118	113	106	100	92
16	89	89	88	86	84	81	77	73	68	63
22	65	65	64	63	61	59	56	53	50	46
32	45	45	44	43	42	41	39	37	34	32
45	32	32	32	31	30	29	28	26	25	23
64	22	22	22	21	21	20	19	18	17	16

2. DEPTH OF FOCUS FOR AN IDEAL LENS

The term "depth of focus" as used throughout this paper refers to the range measured along the axis in the image space that may be traversed without the resolving power measured in the image plane falling below an arbitrarily selected value. It is not to be confused with "depth of field," which refers to the range in the object space for which all point objects are imaged with a radius of the circle of confusion remaining less than or equal to some arbitrarily selected value.

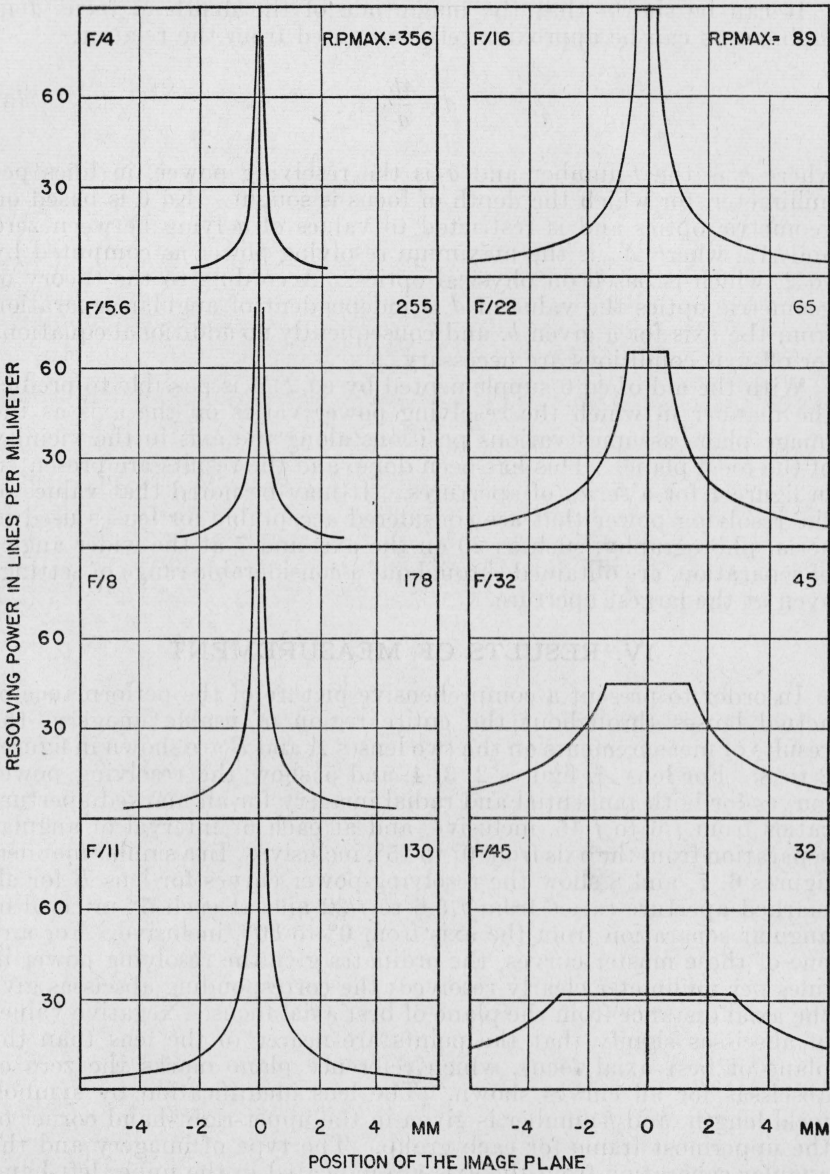


FIGURE 1.—Axial resolving power versus position of the image plane for an ideal lens at several stop openings.

Where the maximum value of the resolving power theoretically possible according to physical optics falls within the scale range of the graphs, a straight-line intercept parallel to the axis of abscissas is shown to indicate that it is not significant to extend higher the two curves, asymptotic to the focal plane, that are derived from geometric optics. Where this maximum falls outside the scale range of the graphs the asymptotic curves are left open at the top but are to be assumed to extend beyond the range of the graph to the theoretical maximum value of the resolving power, which is indicated in the upper right-hand corner of the frame for each stop opening. The zero of abscissas marks the position of best axial focus, and positive values of abscissas indicate positions farther from the lens.

It can be shown that the magnitude of the depth of focus d in millimeters can be approximately computed from the relation

$$d = \frac{4b}{a}, \quad (6)$$

where b is the f -number and a is the resolving power, in lines per millimeter, for which the depth of focus is sought. Eq 6 is based on geometric optics and is restricted to values of a lying between zero and A_m , where A_m is the maximum resolving power as computed by eq 2, which is based on physical optics. According to the theory of geometric optics the value of d is independent of angular separation from the axis for a given b , and consequently no additional equations for off-axis conditions are necessary.

With the aid of eq 6 supplemented by eq 2, it is possible to predict the manner in which the resolving power varies on the axis as the image plane assumes various positions along the axis in the vicinity of the focal plane. This has been done, and the results are presented in figure 1 for a series of apertures. It may be noted that values of the resolving power that are considered acceptable for lenses used in aerial photography, such as 20 on the axis and 7 at the wider angles of separation, are obtained throughout a considerable range of settings even at the largest aperture.

IV. RESULTS OF MEASUREMENT

In order to present a comprehensive picture of the performance of actual lenses throughout the entire region of usable imagery, the results of measurements on the two lenses A and B are shown in figures 2 to 8. For lens A , figures 2, 3, 4, and 5 show the resolving power curves for both tangential and radial imagery for all marked aperture ratios from $f/6$ to $f/45$, inclusive, and at each 5° interval of angular separation from the axis from 0° to 45° , inclusive. In a similar manner, figures 6, 7, and 8 show the resolving-power curves for lens B for all marked aperture ratios from $f/5.6$ to $f/32$ and at each 5° interval of angular separation from the axis from 0° to 30° , inclusive. For any one of these master curves, the ordinates give the resolving power in lines per millimeter clearly resolved; the corresponding abscissas give the axial distance from the plane of best axial focus. Negative values of abscissas signify that the points are nearer to the lens than the plane of best axial focus, which reference plane marks the zero of abscissas for all curves shown. The lens identification by symbol, focal length, and f -number is given in the upper-right-hand corner of the uppermost frame for each group. The type of imagery and the angular separation from the axis are indicated in the upper left-hand corner of each frame. Tangential imagery is signified by the letter T and radial imagery by the letter R .

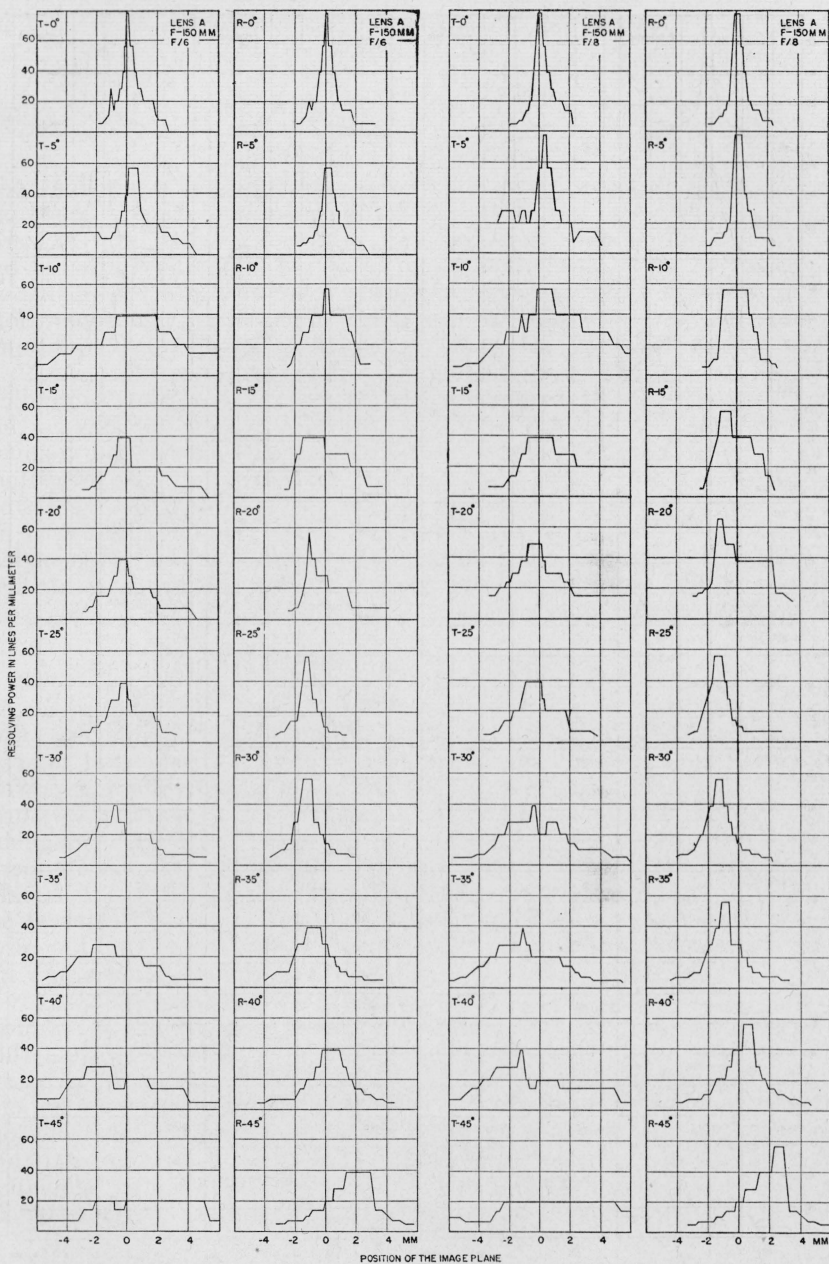


FIGURE 2.—Resolving power versus position of the image plane for lens A at apertures $f/6$ and $f/8$.

The resolving power throughout the region of useful imagery is shown for tangential (T) and radial (R) lines at 5° intervals from 0° to 45°. The zero of abscissa marks the position of best visual focus on the axis at f , and positive values of abscissas indicate positions farther from the lens.

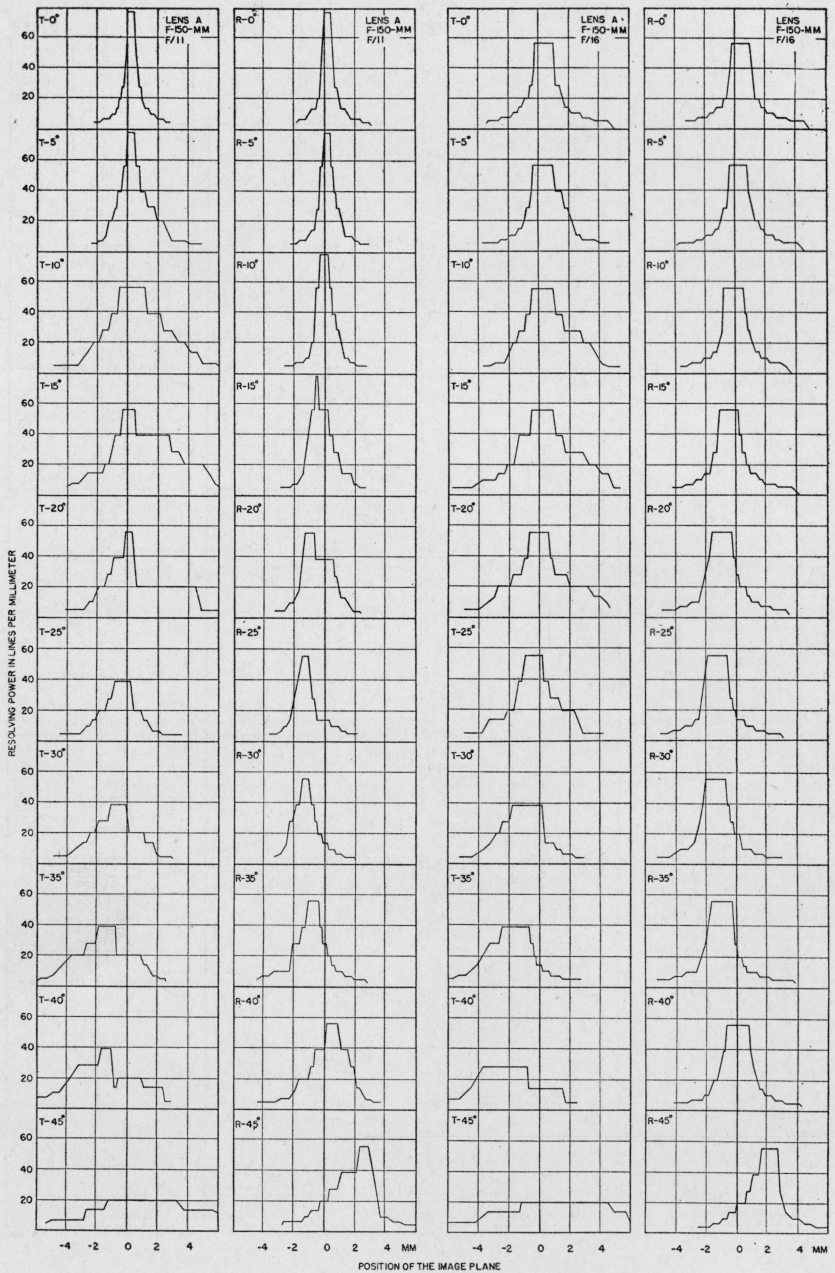


FIGURE 3.—Resolving power versus position of the image plane for lens A at apertures $f/11$ and $f/16$.

The resolving power throughout the region of useful imagery is shown for tangential (*T*) and radial (*R*) lines at 5° intervals from 0° to 45° . The zero of abscissas marks the position of best visual focus on the axis at $f/6$, and positive values of abscissas indicate positions farther from the lens.

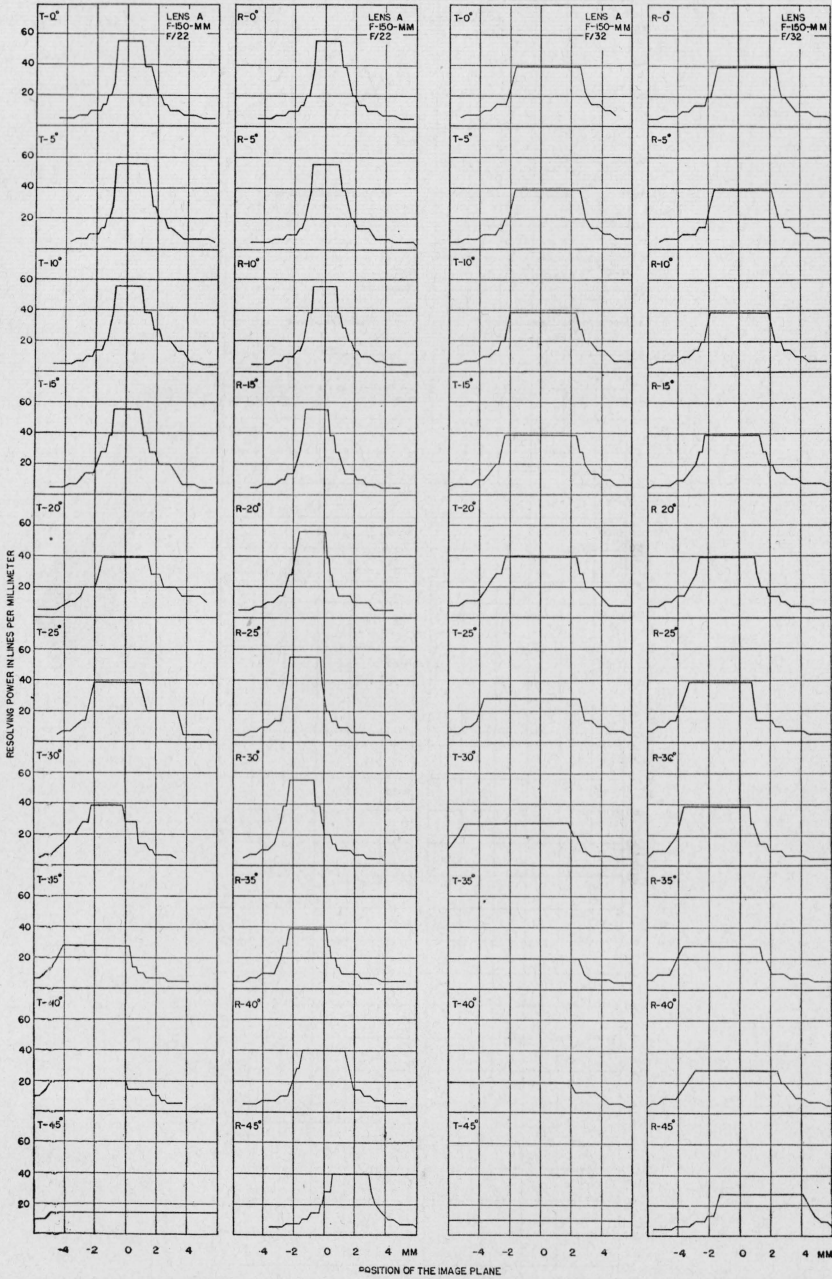


FIGURE 4.—Resolving power versus position of the image plane for lens A at apertures $f/22$ and $f/32$.

The resolving power throughout the region of useful imagery is shown for tangential (T) and radial (R) lines at 5° intervals from 0° to 45°. The zero of abscissas marks the position of best visual focus on the axis at $f/6$, and positive values of abscissas indicate positions farther from the lens.

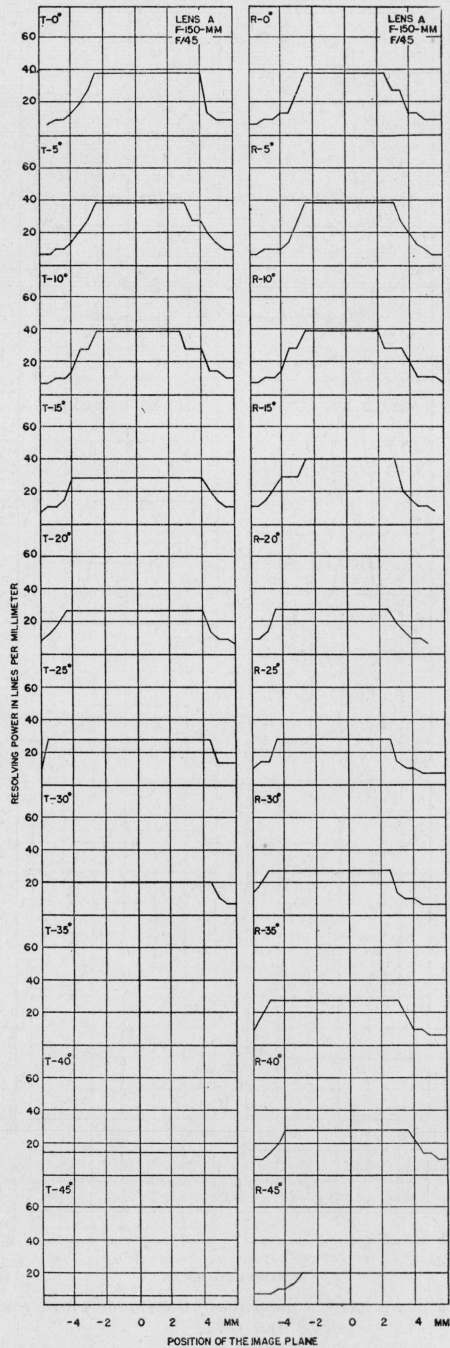


FIGURE 5.—Resolving power versus position of the image plane for lens A at aperture $f/45$.

The resolving power throughout the region of useful imagery is shown for tangential (*T*) and radial (*R*) lines at 5° intervals from 0° to 45°. The zero of abscissas marks the position of best visual focus on the axis at $f/8$, and positive values of abscissas indicate positions farther from the lens.

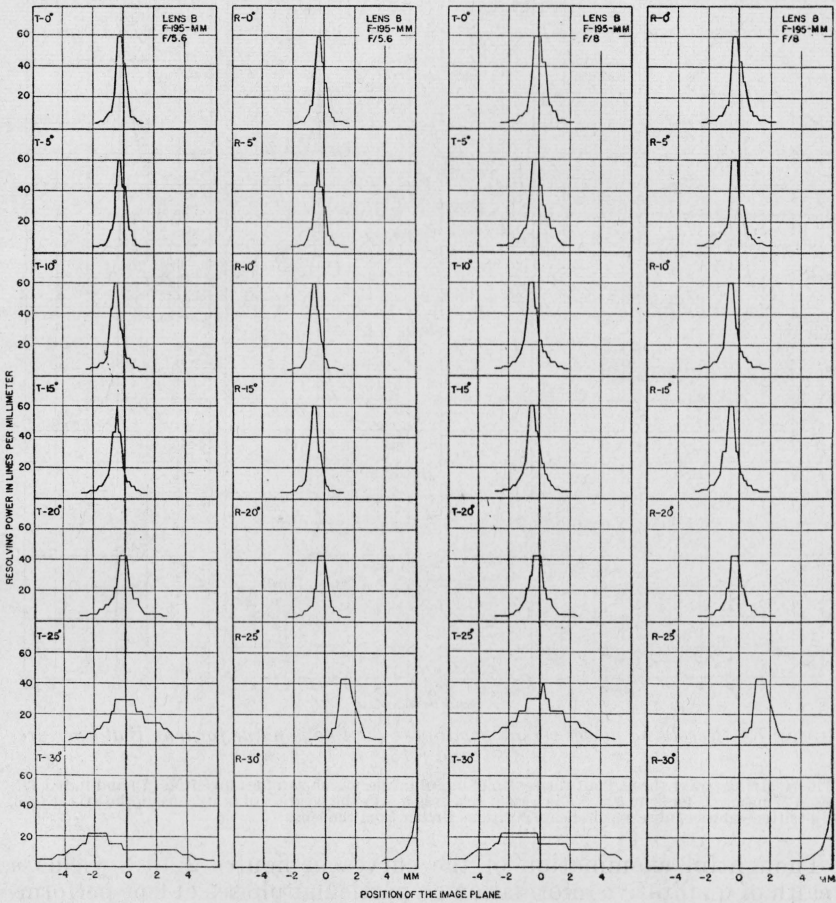


FIGURE 6.—Resolving power versus position of the image plane for lens B at apertures $f/5.6$ and $f/8$.

The resolving power throughout the region of useful imagery is shown for tangential (*T*) and radial (*R*) lines at 5° intervals from 0° to 30°. The zero of abscissas marks the position of best visual focus on the axis at $f/5.6$, and positive values of abscissas indicate positions farther from the lens.

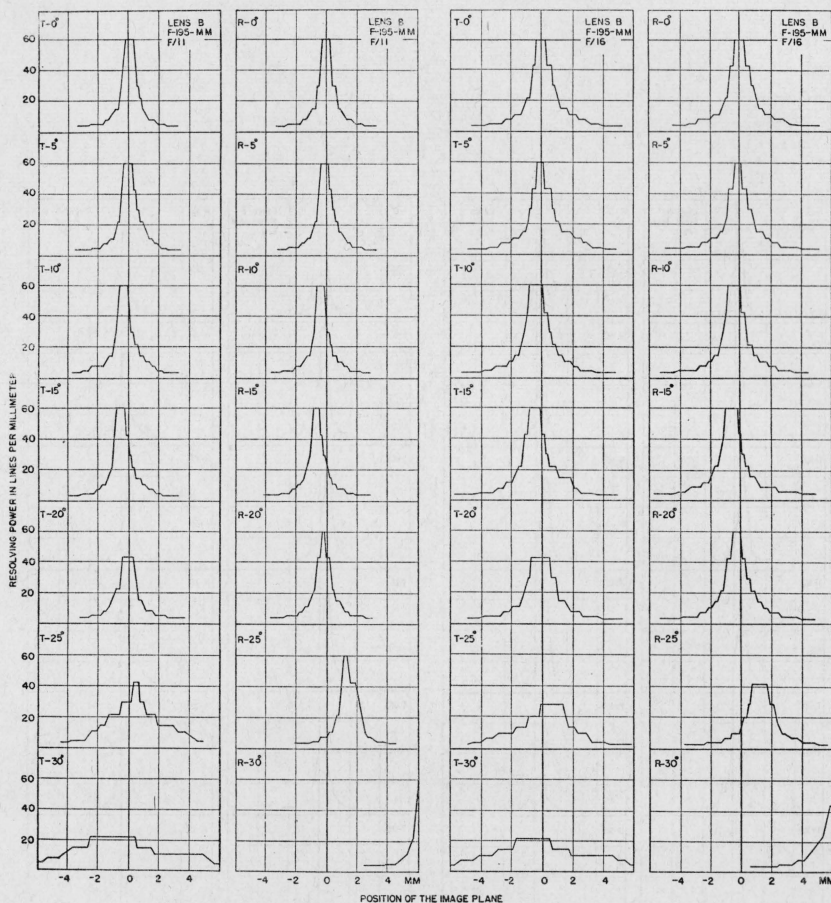


FIGURE 7.—Resolving power versus position of the image plane for lens *B* at apertures $f/11$ and $f/16$.

The resolving power throughout the region of useful imagery is shown for tangential (*T*) and radial (*R*) lines at 5° intervals for 0° to 30°. The zero of abscissas marks the position of best focus on the axis at $f/5.6$, and positive values of abscissas indicate positions farther from the lens.

Thoughtful examination of the curves in figures 2 to 8 yields a wealth of qualitative information on particular phases of lens performance and on the manner in which these separate phases form one coherent whole. However, in view of the complexity of the configuration when viewed as a whole, it is desirable to discuss in separate sections the various aspects of lens performance that are here shown in the integrated form. Chief among these aspects are depth of focus, effect of stop opening, variation with angular separation from the axis, and field curvature. In these sections data derived for lenses *C* and *D* from sets of curves similar to those in figures 2 to 8 (but not shown to conserve space) are presented and discussed in conjunction with the derived data for lenses *A* and *B*. In these discussions, the experimental results are also compared with those predicted from theory.

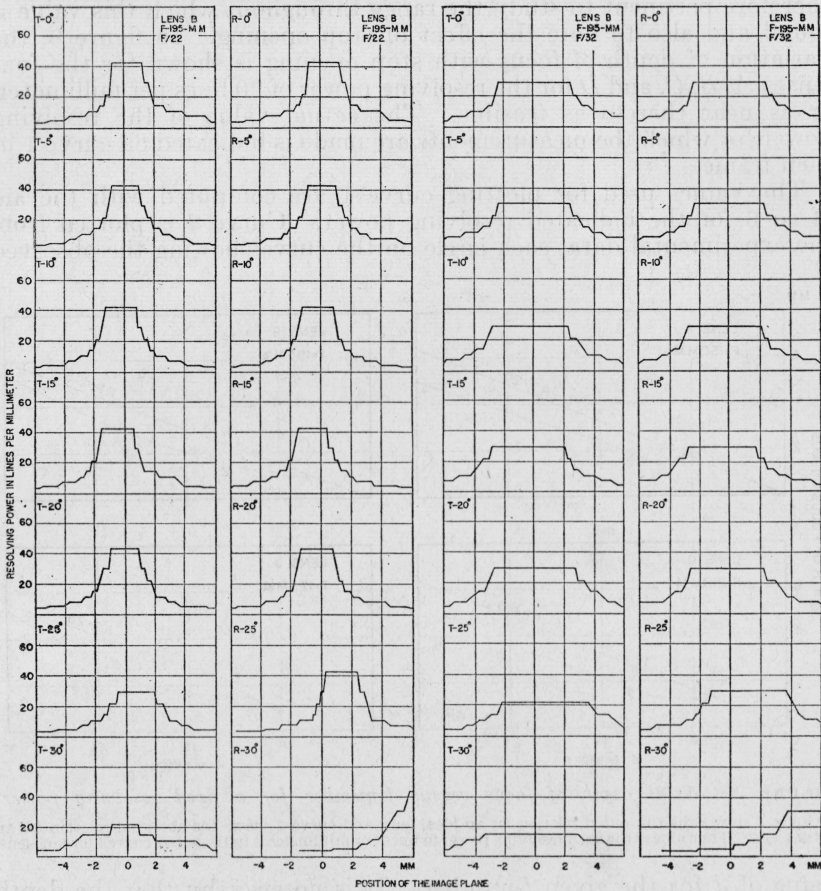


FIGURE 8.—Resolving power versus position of the image plane for lens B at apertures $f/22$ and $f/32$.

The resolving power throughout the region of useful imagery is shown for tangential (T) and radial (R) lines at 5° intervals from 0° to 30° . The zero of abscissas marks the position of best focus on the axis at $f/5.6$, and positive values of abscissas indicate positions farther from the lens.

1. VARIATION IN DEPTH OF FOCUS ON THE AXIS WITH STOP OPENING

When an infinitely distant object is imaged by a lens, the depth of focus is a measure of the range of positions along the optic axis that may be assumed by the image plane without reduction of the resolving power below a specified value. In figures 2 to 8 the depths of focus for any observed resolving power is simply the length of the segment of a straight line parallel to the axis of abscissas cut off by the curve at the selected value of resolving power. Thus the length of this segment for the maximum observed resolving power gives directly the depth of focus in millimeters. However, for comparison purposes, it is preferable to select some value of the resolving power that is attained at each stop opening for the lens considered.

The least axial resolving power allowable under most federal specifications dealing with lens performance is 20 lines per millimeter. It is

therefore pertinent to study the range throughout which this value is found and also to note the effect of stop opening. In figure 9, the variation of depth of focus with stop opening is shown for the four lenses *A*, *B*, *C*, and *D* for the resolving power of 20 lines per millimeter, or as near thereto as feasible. The actual value of the resolving power for which the measurements are made is indicated on curve 1 in each frame.

The values used for plotting curve 1 are computed with the aid of eq 6 for the indicated resolving power. Curve 2 is plotted from the experimental data, each circle on the curve showing the observed

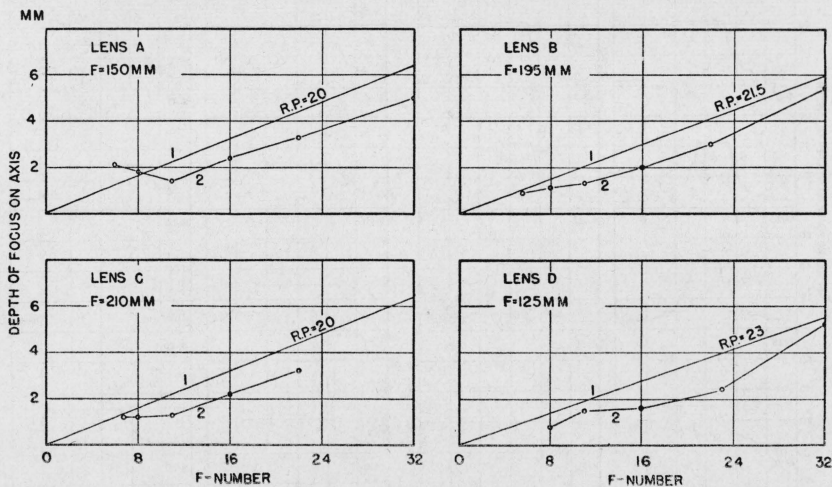


FIGURE 9.—Axial depth of focus versus f -number for a fixed resolving power.

Curve 1 shows the computed relation for an ideal lens, and curve 2 shows the observed relation for an actual lens. The value of the fixed resolving power in lines per millimeter is indicated on curve 1 for each lens.

value of d for the given f -number. It is noteworthy that the depth of focus for an actual lens does not always increase with diminishing aperture. In fact in some instances it may decrease, as is seen in the curve for lens *A*. Here the depth of focus decreases from $f/6$ to $f/11$, and then begins to increase and continues to increase in a linear fashion but at a slope less than that of curve 1. Thus at $f/6$ and $f/8$ the depth of focus is greater than that predicted, whereas at all smaller f -numbers it is substantially less than predicted. The predicted values are not exceeded for lenses *B*, *C*, and *D*. However, the increase with diminishing aperture appears to become more uniform at $f/11$ for *B* and *C*, and at $f/16$ for *D*.

It is clear from these four examples that the increase of depth of focus with diminishing aperture does not proceed in regular fashion until an aperture appreciably smaller than the maximum is reached. The value of the aperture ratio that marks the beginning of regular increase is usually $f/11$, although in some instances it begins as early as $f/8$ and in other instances as late as $f/16$. However, on the basis of many other examples not reported here, $f/11$ is the transition point in the majority of cases studied. In this region of uniform increase, the depth of focus, while increasing steadily with diminishing aperture, is nonetheless lower than that predicted by eq 6 and in most

cases 15 percent or more lower. The anomalous behavior at large aperture ratios, such as is shown by lens *A* at $f/6$ and $f/8$, can only be accounted for by the presence of lens aberrations, which in some instances may so broaden the base of the resolving power curve that values of the depth of focus greater than predicted are found. If the

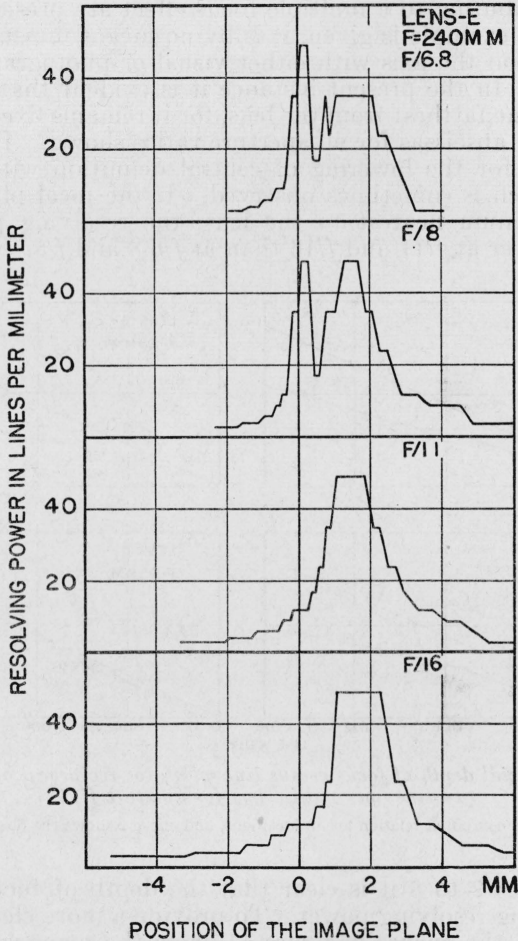


FIGURE 10.—Axial resolving power versus position of the image plane for a lens possessing multiple foci at several stop openings.

The zero of abscissas marks the position of best visual focus on the axis at $f/6.8$, and positive values of abscissas indicate positions farther from the lens.

axial imagery of such a lens as *A* be examined either visually with a microscope or photographically with finer test charts, then it is probable that two or more foci will be seen at full aperture. The axial separation of these foci may vary from a few tenths of a millimeter to more than a millimeter.

This phenomenon has been observed on other lenses and in figure 10, resolving-power curves for lens *E* at $f/6.8$, $f/8$, $f/11$, and $f/16$ show the effect in a striking manner. This lens shows three foci on the axis at

$f/6.8$, drops to two foci at $f/8$ and to a single focus at $f/11$ and $f/16$. It is evident that the outer zones are focused at a point nearer to the lens than the inner zones, the separation of foci in this instance amounting to nearly a millimeter. It is clear from the curves that, if the depth of focus is measured, say at 17 lines per millimeter, the depth of focus will decrease with diminishing aperture so long as conditions contributing to a multiple focus effect are present. Although only this one example is given, it is by no means unusual to find two or more foci on the axis with either visual or photographic means of observation. In the present instance it is evident that the principal focus is the one farthest from the lens, for it remains fixed with respect to the zero of abscissas for all aperture ratios shown. This effect may also account for the lowering of central definition with diminishing aperture which is sometimes observed. If the focal plane is located by the maximum nearest to the lens, the resolving power will be markedly lower at $f/11$ and $f/16$ than at $f/6.8$ and $f/8$.

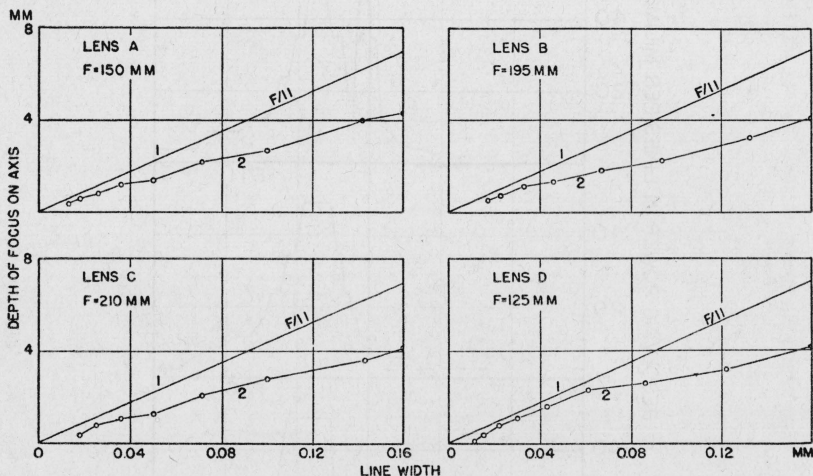


FIGURE 11.—Axial depth of focus versus line width (or reciprocal of resolving power in lines per millimeter) for aperture $f/11$.

Curve 1 shows the computed relation for an ideal lens, and curve 2 shows the observed relation for an actual lens.

From curves 2 to 8 it is clear that the depth of focus diminishes with increasing resolving power. To provide a more clear cut picture of this effect, the curves in figure 11 show the manner in which the depth of focus varies with resolving power for a given f -number, in this instance $f/11$. The reciprocals of resolving power, or line spacings, rather than values of resolving power are plotted as abscissas in order that the theoretical curve computed from eq 6 appear as a straight line instead of a rectangular hyperbola. Curve 1 shows the variation predicted and curve 2 shows that actually found. Aside from the observed values of depth of focus being lower than the predicted, there are no important deviations from theory. The curves do show the greater freedom in selection of a focal plane that exists for the lower resolving powers.

2. VARIATION IN RESOLVING POWER ON THE AXIS WITH STOP OPENING

The upper limit of resolving power, expressed in lines per millimeter, is determined by aperture ratio and wavelength of the image forming light. The capacity of a lens to yield this maximum resolving power is in practice impaired by lens aberrations. In the present instance, the patterns of the test chart are not sufficiently fine to show variations in the maximum resolving power at the larger stop openings. This is evident when it is noted that the maximum resolving power on the test chart for lens *A* is 78 lines per millimeter, which is higher than can be expected for $f/22$ and lower than predicted for $f/16$. For lens *B*, the test-chart maximum is 56, which is greater than the predicted value at $f/32$ and less than predicted at $f/22$.

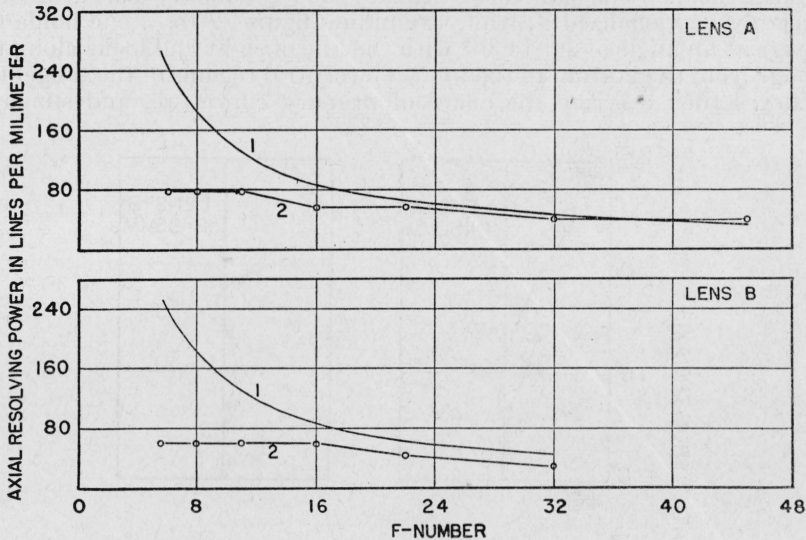


FIGURE 12.—Maximum axial resolving power versus stop opening.

Curve 1 shows the computed relation for an ideal lens for a wavelength of 575 millimicrons. Curve 2 shows the observed relation for an actual lens.

However, despite these limitation in the test-chart scale, some information on the change in resolving power with stop opening can be obtained from the curves in figures 2 to 8. To facilitate study, the maximum observed resolving power is plotted against f -number as curve 2 in figure 12 for lens *A* and *B*. Curve 1 in each frame shows the maximum theoretical resolving power.

For lens *A*, it is evident that the maximum fixed by the test chart is obtained for $f/6$, $f/8$, and $f/11$. However, the resolving power drops to 56 at $f/16$, which drop can be attributed to lens aberrations. The value of 56 is still maintained at $f/22$, and since the theoretical is only 65, it can be stated that the lens aberrations definitely affect the resolving power less at $f/22$ than at $f/16$. The two curves are nearly in coincidence at $f/32$ and $f/45$, thus clearly showing the drop in resolving power with diminishing aperture as well as demonstrating that the drop in resolving power at small apertures results from

theoretical limitations based on aperture rather than on the effect of lens aberrations.

In the case of lens *B*, the limitations imposed by the test chart preclude any effect becoming noticeable for most of the range; however, it is clear that lens aberrations are effective at $f/22$ and $f/32$ in preventing the lens from performing as predicted by theory.

3. EFFECT OF FIELD CURVATURE

It is apparent on examination of a given series of curves at a specified stop opening, for either tangential or radial imagery, that the position of maximum resolving power occurs at different distances from the position of best axial definition for the various angular separations from the axis. This effect is a result of curvature of the image field. The curves of primary and secondary curvature can readily be visualized if, while examining figures 2 to 8, one holds the page at an angle of 20° to 30° with the line of sight and looks along the page from the bottom to the top. The central regions of the tangential curves then describe the curve of primary curvature, and similarly

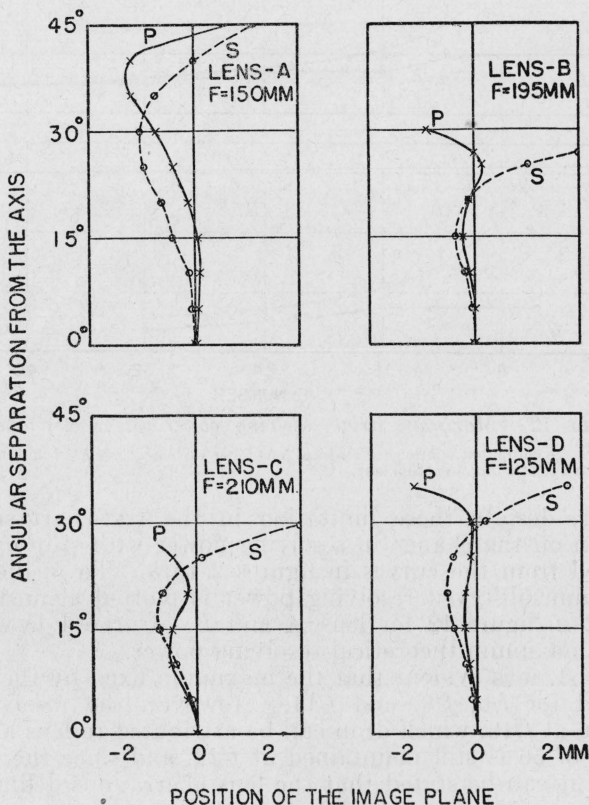


FIGURE 13.—Field curvature.

Curve *P* shows the primary curvature and is the locus of the positions of maximum resolving power for tangential lines at the indicated angular separations from the axis. Curve *S* shows the secondary curvature and is the locus of the positions of maximum resolving power for radial lines at the indicated angular separations from the axis. The zero of abscissas marks the position of best axial focus and positive values of abscissas indicate positions farther from the lens.

the central regions of the radial curves show the curve of secondary curvature.

The primary and secondary curvatures for lenses *A*, *B*, *C*, and *D* are shown in conventional form in figure 13. The curves, as drawn, represent an average value of the field curvature for several apertures and consequently do not portray precisely the observed field curvature at any single aperture. It was noted in the course of this investigation that the shape of the field curves changes appreciably when going from the largest stop opening to the smallest. However, it was not considered worthwhile to show this change in detail.

It is this effect produced by field curvature that makes it pointless to search out an image plane that yields say 200 lines per millimeter on the axis, because so placing the image plane automatically fixes the resolving power obtainable for the 30° region at 14 lines per millimeter or less. It is clear from the curves in figures 2 to 8, and 13 that no single image plane can include the position of maximum resolving power for all angular separations from the axis for either type of imagery. Consequently, selection of an image plane that will yield values of the resolving power sufficient for good usable photography in all parts of the image plane for both types of imagery is preferable to selection of the plane of best axial imagery. It may also be noted that this shift of the maxima of resolving power for the various angular separations from the axis justified setting the upper limit of the test-chart patterns to exceed that of the average emulsion but not necessarily to exceed the theoretical resolving power of the lens at the larger stop opening.

4. CHANGE IN DEPTH OF FOCUS WITH ANGULAR SEPARATION FROM THE AXIS

Examination of the curves in figures 2 to 8 shows that for a given *f*-number and specified resolving power the depth of focus is not generally constant. This behavior is markedly different from that which would be manifested by an ideal lens for which the depth of focus is constant under these conditions. Accordingly, curves illustrating this lack of constancy in depth of focus for the lenses studied are shown in figure 14. The resolving power in each case is 20 lines per millimeter or as near thereto as feasible, the actual value being indicated. The variation of depth of focus with angular separation from the axis is shown for a series of *f*-numbers for each of the lenses *A*, *B*, *C*, and *D*. The theoretical depth of focus on the axis is marked by a short line projecting from the axis of ordinates. It must be borne in mind that the ordinates for any value of the abscissas represent only the range throughout which the particular resolving power for that type of imagery is observed, and the curves do not show the space relationship of these ranges with respect to one another. It is possible to draw curves, showing the depth of focus, that preserve the space relationships but since this would involve the effect of field curvature, the change in depth of focus with angle would be somewhat obscured.

It is noteworthy that of these four examples only lens *B* preserves a near constancy of depth of focus for tangential and radial lines with angular separation from the axis, and that even here there is an abrupt change between 20° and 25° . Since this change is more pronounced at the larger stop opening, it is probable that the increase

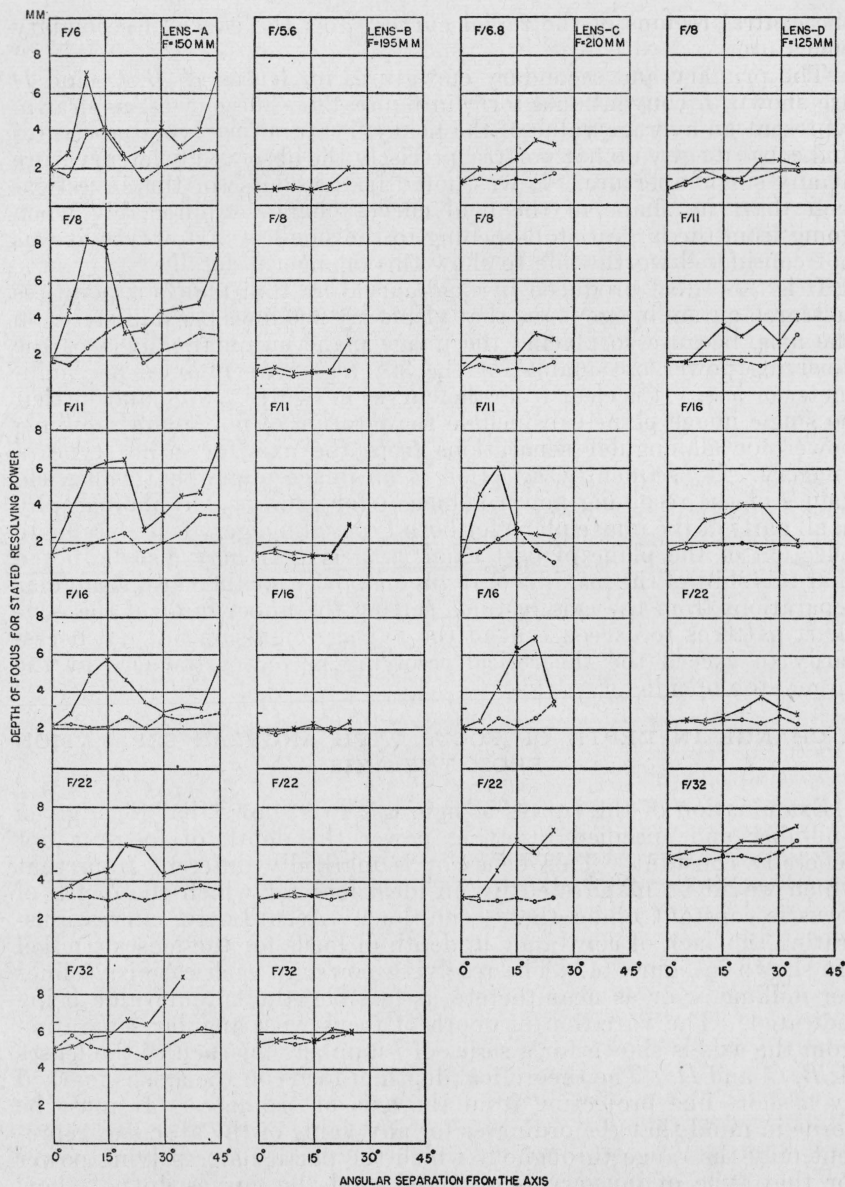


FIGURE 14.—Depth of focus versus angular separation from the axis for a fixed resolving power for a series of stop openings.

The value of the resolving power is 20 lines per millimeter for lenses *A* and *C*, 21.5 for lens *B*, and 23 for lens *D*. The solid curve shows the depth of focus for tangential imagery, and the dotted curve shows the depth of focus for radial imagery. The short line projecting from the axis of ordinates shows the computed depth of focus for an ideal lens.

in depth of focus is a consequence of vignetting by the lens boundaries which produces a sharp reduction in effective aperture between 20° and 25° . Too, it may be noted that in the region of 0° to 20° the theoretical maximum is not exceeded. Wide variations in the depth of focus with angle are shown by lenses *A*, *C*, and *D*, and the variations for tangential lines make the greater changes. Since these changes in many instances carry the depth of focus above the theoretical maximum it is reasonable to suppose that this is another manifestation of the multiple focus effect discussed in section 1.

The fact that the depth of focus for tangential lines is usually greater than that for radial lines is probably a consequence of the asymmetric use of aperture for tangential imagery, thus permitting the aberrations to increase the depth of focus at the expense of a lowered maximum observable resolving power.

5. CHANGE IN MAXIMUM RESOLVING POWER WITH ANGULAR SEPARATION FROM THE AXIS

Examination of the curves shown in figures 2 to 8 shows that the maximum resolving power decreases with increasing angular separation from the axis. This effect is more pronounced for tangential than for radial lines, although definitely present in the latter. This effect is compounded from lens aberrations and limitations set by aperture ratio. For the larger stop openings the decrease evident from the curves arises mainly from aberrations because the upper limit set by the stop opening is well above the upper limit set by the test charts. The variation in the maximum value of resolving power with angular separation from the axis is shown graphically in figure 15. The solid line curves represent the variation in maximum resolving power with angle as computed with the aid of eqs 4 and 5. The broken curves are the results of observation.

It is interesting to note that, save for one exception, the resolving power decreases monotonically from a maximum on the axis to the last observed value for both tangential and radial lines. However, the resolving power for tangential lines decreases more rapidly than does the resolving power for radial lines. This behavior is of course predicted by theory, but it is interesting to note that this behavior is present for those stop openings where the least resolving power predicted for any angle is nonetheless higher than the upper limit of the test chart, as can be seen from the curves for $f/6$ and $f/8$. At $f/11$, the effect of diminishing aperture is evident, particularly for tangential values, although even here it is clear that aberrations are chiefly responsible for the failure of the lens to yield full theoretical resolving power. At $f/16$, the limits imposed by stop opening become more evident, the theoretical and observed curves are closer together and their similarity becomes more pronounced. At $f/22$, the effects of aberrations are practically nil and the two curves nearly coincide. This close coincidence of the two curves continues through $f/32$ and $f/45$.

From the study of these curves it is evident that lens aberrations are of primary importance in limiting the maximum resolving power of lens *A* for the aperture ratios from $f/6$ to $f/11$. From $f/16$ on, the maximum values of the observed resolving power conform more and more closely to the values predicted by theory; thus these observations tend to validate the accuracy of eqs 4 and 5.

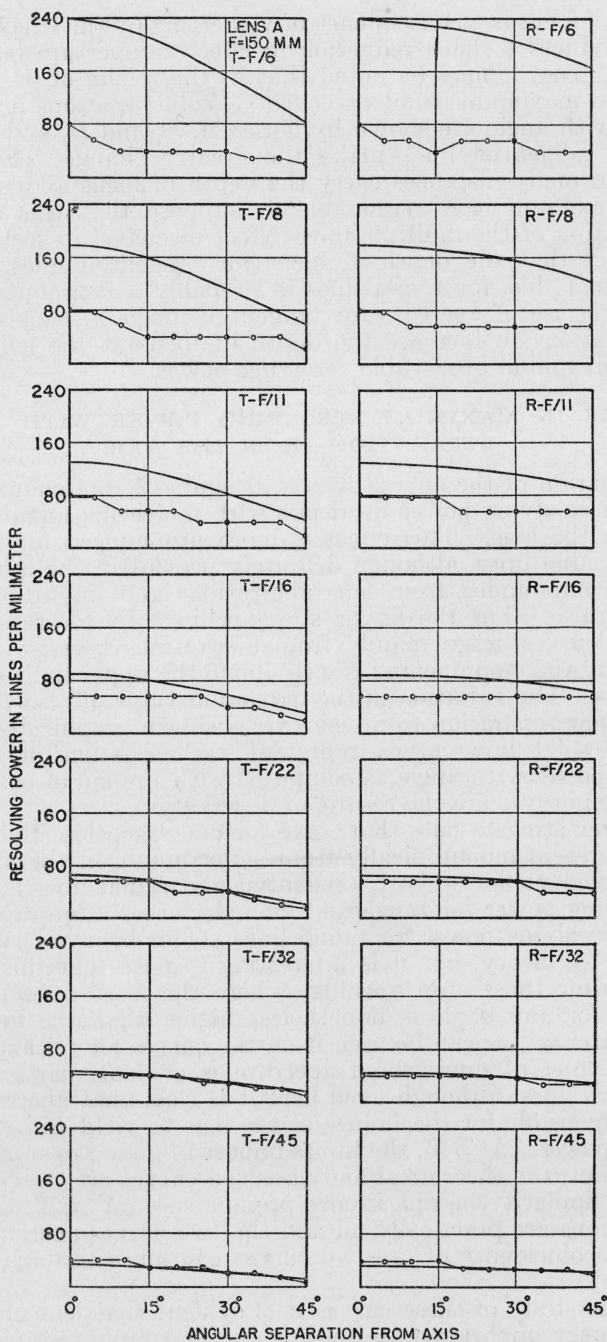


FIGURE 15.—Maximum resolving power versus angular separation from the axis for a series of stop openings.

The solid curve shows the computed relation for an ideal lens, and the broken curve shows the observed relation for an actual lens. *T* signifies tangential imagery and *R* radial imagery.

6. VARIATION OF RESOLVING POWER IN A GIVEN IMAGE PLANE WITH STOP OPENING

A general improvement in definition throughout the image plane is frequently encountered when the imagery obtained with a lens set at a small stop opening is compared with that obtained with the same lens set at a larger stop opening. At first thought, this behavior appears to be at variance with the fact that the resolving power of a lens for any given part of the image plane is a maximum at the largest stop opening. However, because of curvature of the image field (discussed in section 3) the image plane for an actual lens cannot usually be so placed as to contain all the resolving power maxima for all angular separations from the axis. On the contrary, a given image plane can include only a few of the resolving-power maxima for a lens set at maximum stop opening; and, as is evident from examination of the master curves shown for lens *A* at $f/6$ in figure 2, the small depth of focus present for maximum resolving power at the various angular separations from the axis further serves to limit the number of resolving-power maxima obtainable in the image plane.

If, as is the case for airplane cameras, the image plane is maintained at a fixed distance from the lens, which distance is established as yielding best average definition at full stop opening, it is clear that when a smaller stop opening is used the depth of focus for each maximum increases. Consequently, there is greater likelihood of the given image plane including more resolving-power maxima than it did at the full stop opening and, as a result, the definition considered throughout the image plane will show improvement. As a matter of fact, some improvement is likely even if more maxima are not included because the increased depth of focus for any observed resolving power makes it probable that some regions will be benefited by an increase in resolving power even if the maximum is not reached. The manner in which this effect is operative can be seen from the curves shown in figures 2 to 8. For lens *A*, if one selects an image plane 0.20 mm nearer the lens than the plane of best axial focus, the resolving power for tangential lines at 5° from the axis increases from 28 to 56 lines per millimeter when the aperture is reduced from $f/6$ to $f/11$. Similar gains can be noted in other parts of the field.

This improvement does not continue indefinitely with diminishing stop opening. For lens *A*, reducing the f -number below $f/22$ causes a general decrease in resolving power throughout the image plane. This arises from the fact that the limitations set by aperture ratio (described in section 2) becomes noticeable. For apertures between $f/6$ and $f/22$, the upper limit of the resolving power for the various regions of the image plane is set preponderantly by lens aberrations; but for $f/32$ and $f/45$, the upper limit is set by aperture ratio.

It must be mentioned that there are additional reasons for the betterment of photographic quality with diminishing stop opening. Chief of these is the reduction of the large variation in effective exposure over the photographic plate which otherwise would be produced by vignetting. The difference in relative illumination is of course much less when the diaphragm stop is the only limiting aperture.³

WASHINGTON, November 14, 1944.

³ J. Research NBS 29, 233 (1912) RP1498.